Effect of a diffuser on the power production of Ocean Current Turbines

J. Reinecke
Stellenbosch University, Stellenbosch, South Africa

Centre for Renewable and Sustainable Energy Studies

Abstract
Ocean current turbines (OCTs) are hydropower turbines that involve the extraction of kinetic energy from ocean currents. The marine current resource has a major advantage over other renewable energy resources in that it is essentially non-intermittent and predictable over long time periods.
The purpose of the study is to investigate the increase in power density of an existing model ocean current turbine, by use of a geometrically optimized curved plate diffuser. A single curved plate diffuser with area ratio of 3.29 was designed. By characterizing the diffuser shape as a B-spline defined by four variables. A two-dimensional CFD analysis was created as function evaluations for a Latin Hyper Cube Design of Experiments. A Support Vector Regression metamodel was constructed from the DOE and optimized. The model predicted a maximum Cp of 1.672.The diffuser was manufactured and tests conducted in a towing tank facility at a flow speed of 1.5m/s. Results showed an increase in turbine peak power from 383 W (Cp =0.43) for the bare turbine to a measured 1512 W (Cp = 1.74) for the turbine with the optimized diffuser. This represented an increase in power production by a factor of 4.05.

Keywords: Ocean current turbine, Renewable energy, Diffuser, Support vector regression, CFD.

1. Introduction

Ocean and tidal currents are renewable energy sources being investigated for kinetic energy extraction. Water having a density of approximately 830 times that of air allows for greater kinetic energy extraction over that of wind at similar flow speeds and rotor size. Given a suitable site of concentrated flow and high speed velocities, ocean current turbines can offer up to four times the energy intensity of a good wind site and 30 times the energy intensity of a solar plant in the Sahara Desert (Fraenkel 2007). Ocean currents are regular, and their strength and directional frequency can be predicted. This allows for a degree of availability which is not often encountered within renewable energy (Batten et al. 2008).

Low kinetic energy density affects the economic feasibility and choice of installation sites of OCT technology (Gaden & Bibeau 2010). This investigation then studies the use of diffusers to increase the kinetic energy density at the rotor plane of a existing model OCTs. Continuing from a previous study that achieved a factor increase in turbine power of 1.85 (Grobebelaar 2008) through use of a straight wall diffuser, our aim was to increase the the power generated by at least a factor 2.

The purpose of the study is to investigate the increase in power density of an existing model ocean current turbine by use of a geometrically optimized curved plate diffuser for enhanced cost effectiveness. A single curved plate diffuser with area ratio of 3.29 (apparent area of diffuser over the rotor swept area) was designed.

1.1. Literature Review
Satellite altimetry estimates the amount of power dissipation in kinetic energy onto the north west continental shelf of Europe to be 219 GW (Egbert & Ray2001). Some estimates place Canada's potential at 50 TWh/y and (Bedard et al. 2007) and recently it's been suggested

that the initial resource estimation of 12 TWh/y (1.4 GW) for the UK is incorrect and a more representative estimate of 20 GW is suggested for the extractable power around the British Isle's (Mackay 2007). Currently resource assessments are being conducted by Eskom on the Agulhas current. Recent findings point to average velocities of 1.63 m/s up to a peak velocity of 2.5 m/s and estimates a potential resource of 600 GW (Mgwatyu 2009) of power.

Extracting these large amounts of kinetic energy is accomplished by implementing of existing wind turbine theory to design OCTs as they are similar in operation and design (Rourke et al. 2010). Accordingly horizontal and vertical axis turbines make up the two main categories currently being developed (Rourke 2009; Rourke et al. 2010). The largest turbines currently nearing the commercial phase are horizontal axis turbines. Table 1 highlights the two largest turbines currently deployed.

Table 1: Current OCTs with details

Device	Illustration	Features	Status
SeaGen		Twin two bladed Ø 16m rotors. Rated 1.2 MW at 2.4 m/s.	1.2 MW Full scale Prototype installed April 2008
Ak-1000		Twin three bladed Ø 18m rotors. Rated 1 MW at 2.64 m/s	1 MW Full scale Prototype installed August 2010.

Investigations using a diffuser to increase the kinetic energy density at the turbine was first conducted in wind turbines. Various diffuser shapes including a shroud have been investigated in (Igra 1981). Foundings from his experiments focused on using annular airfoils and straight wall diffusers with bleed slots to increase the kinetic energy. He found that for a straight wall diffuser with expanding inclination angle of 12.6°a increase in power of a factor 2.9 was recorded at a diffuser area ratio of 2. The experimental diffusers had a length of 6.8 times the rotor diameter with limited tip clearance.

In (Matsushima et al. 2006) a straight wall diffuser with a flanged end piece was able to demonstrate a increase in power by a factor 2.4 experimentally that differed from the factor 5 power increase prediction from CFD. Grassmann (Grassmann 2003) designed a compact diffuser using annular airfoils that included a large tip clearance. This larger clearance allowed around the rotor to influence the low pressure region behind the rotor and also delay the onset of boundary separation. Increase in power of a factor 2 was predicted by CFD but a power increase factor of 1.5 was measured experimentally at a diffuser area ratio of 2.25.

Diffuser augmentation of wind turbines never realised at commercial level due to the variance in loading conditions that needed to be accounted for by the support structure that implied a large material cost rendering diffuser augmented wind turbines economically

infeasible. However Ocean currents and tidal streams have little variances in flow speeds and are directional and thus diffuser augmentation in OCTs are being explored anew.

A recent study using a optimized straight wall diffuser for river kinetic turbines predicted an increase in power by a factor 3.1 at a diffuser area ratio of 1.56 using a CFD model (Gaden & Bibeau 2010). This was however not validated experimentally.

Investigation into diffuser augmentation of OCTs was conducted by Grobbelaar (Grobbelaar 2008) utilizing a optimized straight wall diffuser. CFD studies on a 0.4 m radius rotor with a optimized straight wall diffuser of radius 0.726 m showed a increase of power by a factor 2. In tests conducted on the diffuser augmented turbine, a power increase factor of 1.85 was achieved at a diffuser area ratio cost of 3.29.

In order to quantify the gains of using support vector regression in diffuser design, a new diffuser of similar geometric envelope to (Grobbelaar 2008) was designed and tested using the same model OCT rotor.

2. Theory

Extracting the kinetic energy from a free flowing fluid is limited by the Betz law (Betz 1920). It states that the maximum extractible power by a turbine from a free stream is 59.3 %.

2.1. Betz's Law

This occurs when kinetic energy is removed from the fluid that in turns causes a change in the upstream pressure and slows down the fluid velocity downstream. This change in pressure causes some fluid to divert around the rotor and thus the effective area of the stream tube upstream shrinks compared to the rotor area. Behind the rotor the pressure drops and a expansion in the stream lines occurs. Due to conservation of mass the ratio of stream tube areas can also be expressed as the ratio of velocities far upstream, at the rotor plane and in the wake. A factor relating the velocities is called the induction factor. It follows from the conservation of momentum equation that the velocity passing through the turbine is the average of the upstream and downstream velocities.

$$u = V_0(1 - a) \tag{1}$$
$$u_1 = V_0(1 - 2a) \tag{2}$$

Where u is the axial velocity at the rotor plane, V_0 the free stream axial velocity far upstream and u_1 the axial velocity downstream of the rotor plane. a is the induction factor and varies between 0 and 1. When we apply axial momentum conservation and assume frictionless incompressible flow, a relation can be derived for the coefficient of power C_p that relates the shaft power to the available power.

$$C_p = 4a(1 - a)^2 \tag{3}$$

The derivative of this equation shows that a maximum $C_p = 16/27 = 0.593$ is achieved when $a = 1/3$. This corresponds to the Betz law that states that the maximum amount of power extractable from a stream tube is 59.3 % of the available power.

An expansion on the Betz law to include fluid dynamic components near the rotor plane has been theorized by (Jamieson et al. 2008) and (Werle & Presz 2008) showing that exceeding the Betz limit is possible. Gaden (Gaden & Bibeau 2010) attributed exceeding the Betz limit to the upstream effect a diffuser has by increasing the mass flow through the rotor and hence the velocity. Now a numerical model of the rotor and diffuser needed to be created to conduct optimization experiments.

2.2. Numerical Model

To investigate the effect of a diffuser on the performance of the turbine rotor, a rotor model was specified for the CFD applications. A pressure jump formulation was selected that modelled the rotor as a discontinuous pressure jump thus simulating the extraction of the kinetic energy. The formulation used is presented in equation 4.

$$\qquad (4)$$

Here   is the pressure jump across the rotor and   the water density taken as 998 kg/m^3. A two dimensional axisymmetric grid with tri-pave elements was used to represent the flow domain. After grid dependency tests were conducted a grid with mesh size of 42 464 cells and a worst element skewness of 0.48 and area ratio of 4.8 existed. A velocity inlet and pressure outlet boundary conditions were selected. The inlet flow speed was taken as 1.5 m/s corresponding to the experimental towing speed. The mesh was created in Gambit and the solver used ANSYS Fluent. The flow domain extended 2.4 m upstream of the rotor and 6.4 m downstream of the rotor. From the rotor axis the domain extended 2.8 m in the radial direction.

To validate the the pressure jump formulation the rotor model performance was compared to standard one dimensional wind turbine theory presented in (Hansen 2008) for a induction factor range   and to the modified Glauert empirical relation as suggested by (Buhl & Buhl 2005) for   . Two turbulence models where used namely the k-ν Realizable and k-ω Standard models. The results are show in figure 1.
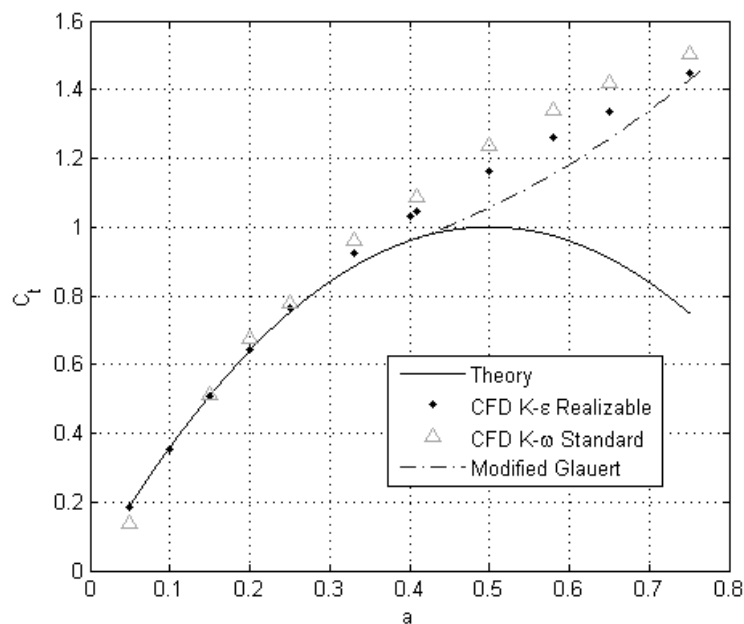

Figure 1: C$_t$ vs. a graph comparing CFD rotor formulation to existing theories.

From the figure it can be seen that the k-ν model outperformed the k-ω model. The pressure jump model implementing the k-ν model gave a maximum prediction error in   of 4% at   . Thus validating the use of the rotor model and chosen grid specifics and turbulence model.

3.   Diffuser Optimization

The use of metamodels in optimization has growing significance in highly non-linear engineering applications as it reduces the computational cost associated with gradient methods such as sequential quadratic programming (SQP) and direct methods such as particle swarm optimization for problems involving 20 or less variables (Lee et al. 2008; Viana 2009). In order to create a metamodel, a design of experiments is conducted from which responses from a complex engineering code (CFD, FEM etc.) is acquired. This is done by following some DOE configuration that effectively varies the design variables in the optimization problem to gain insight into the design variable relationships. The goal of the DOE is to gather as much information with minimal analysis so as to give a accurate representation of the design space.

3.1. Metamodeling

Metamodels effectively reduce high cost function evaluations such as CFD or FEM models to a set of mathematical formulations over the design space. This gives metamodelling the ability to investigate various relationships between variables across the design space and allows recalculation of the optimum for various constraints that can be added after the metamodel has been fitted, making it a versatile method (Clarke et al. 2005). Other metamodeling techniques used is response surface (RS) modelling, Kriging and radial basis functions (RBF). However RS modelling assumes a underlying form of a polynomial nature for the design and is ineffective when highly non-linear design space approximations are required compared to support vector regression (SVR). Kriging and RBFs use a black box approach to the optimization problem and assumes no underlying form. The SVR technique does not use a black box approach and neither assumes a underlying form.

Mathematically, if the inputs to the actual computer analysis are supplied in vector x, and the outputs from the analysis in vector y, the true computational code evaluates:

$$y = f(x) \tag{5}$$

where $f(x)$ is a complex engineering analysis function (CFD, FEM etc.). The computationally efficient metamodel approximation is:

$$\hat{y} = g(x) \tag{6}$$

such that

$$y = \hat{y} + \varepsilon \tag{7}$$

where ε includes both approximation and random errors. The basic formulation of the SVR algorithm can be expressed as:

$$\hat{y} = \sum_{i=1}^{p} (a_i - a_i^*) K(x_i, x) + b$$

Where $(a_i - a_i^*)$ and b are obtained during the fitment process, $K(x_i, x)$ is the kernel function where x_i are various training points from the DOE and x is the point in the design space where the SVR model is to be evaluated.

3.2. Optimization Problem

The current optimization problem is best described at the hand of the diffuser representation and its design variables. The diffuser shape to be optimized was a single curved plate geometry approximated by using a B-spline that is characterized by four design variables. The curved plate diffuser and straight wall diffuser is shown in fig. 2.
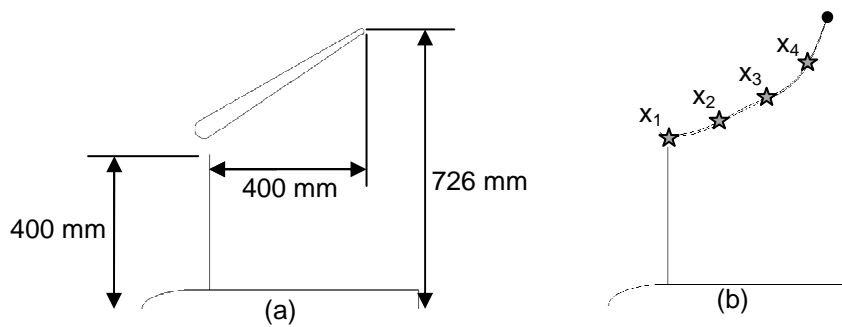
Figure 2: (a) Diffuser dimensions as defined in (Grobbelaar 2008), (b) Curved plate diffuser with variable points

In fig. 2 (b) x_1,x_2,x_3 and x_4 represent the design variables that are horizontally equally spaced 100 mm from each other starting at the rotor plane. The dot to the right of x_4 represent a fixed position of 726 mm that is unchanged during the optimization procedure. All the design variables had fixed axial locations but was allowed to vary in the radial direction thus the problem consisted of four design variables. Monotinicity constraints where also applied to prevent negative gradients along the B-spline.

The optimization problem can then be formulated as:

$$\textbf{Maximize:} \tag{8}$$

$$\textbf{Subject to:} \tag{9}$$
$$\tag{10}$$
$$\tag{11}$$
$$\tag{12}$$

Note that 0.415 m is specified as the lower limit for   so that at a minimum radial gap of 0.015 m existed between the rotor tip and diffuser. This minimized the risk of rotor brakeage in operation.

3.3. Design of Experiment

A latin hyper cube (LHC) design of experiments (DOE) was used to generate 110 training points and 25 test points. Each point in the DOE represents a single CFD analysis with unique values of the design variables.

A 2D- axisymmetric grid was used with the diffuser geometrically represented by a B-spline. The mesh was generated using Gambit and the solver used Fluent. In order to process the points in parallel the use of text command scripts or journal files where used to initiate and complete all CFD analysis. By using a Python script that changed design variable values in the parameterized Gambit journal file the DOE could be completed in parallel on a high speed computing cluster.

Computation of the power coefficient (   ) from the CFD analysis were accomplished by recording the mass average pressure difference (   ) across the rotor plane and the axial velocity at the rotor plane (   ). Using these two variables the thrust force that results across the rotor plane due to the extraction of kinetic energy from the fluid could be determined. For the CFD power coefficient (   ) is then defined as follows:

_____

3.4. Support Vector Regression Modelling

The110 training points analyzed and the corresponding responses was used to fit the SVR model. A open issue in SVR creation is choosing the values used for the insensitivity

parameter $\mathtt{e}$, the regularization parameter C and the Gaussian RBF kernel function's radius parameter $\mathtt{s}$. In order to specify these variables a parameter analysis was used where $\mathtt{e}=$ 0.00001 was chosen as the best insensitivity value from various analysis.

To determine the correct values of C and $\mathtt{s}$, both where allowed to vary between a range of 0 to 200 and 0 to 10 respectively. For each specific C and $\mathtt{s}$ cross validation was applied. This process fits the model to 109 training points. It then calculates how well the model predicts the value of the 110th training point and calculates the root mean square (RMS) of the error. This method was conducted for all 110 points and a RMS error of all the prediction errors recorded.

In addition the absolute average error (AAE) was also calculated but in a different way to the cross validation method. For a given C and $\mathtt{s}$, the SVR model was fitted to all 110 points and the AAE calculated between each point's approximation value and actual CFD response. After fitment was completed and the AAE calculated for the training points, the test points where used to calculate the AAE between the model's prediction of the the test points and the model approximations. The results showed that the best values for C and $\mathtt{s}$ where 60 and 0.047 respectively and these were also chosen for the final SVR model.

The numerical code Matlab was used to implement the SVR model along with the toolbox developed by Viana in (Viana 2009). After creating the final SVR model the built-in optimizer of Matlab was used to find the optimum. After each optimum was reached in Matlab it was validated by conducting a CFD analysis and the CFD value added to the original 110 DOE points. This continued until convergence in the C_p value was reached. After 12 iterations convergence was achieved and a final optimum in the diffuser design emerged. The optimum values are shown in table 2.

Table 2: Details of optimum diffuser as determined by SVR

C_p	C_d	x_1	x_2	x_3	x_4
1.672	1.728	0.426	0.4463	0.4984	0.5480

Here C_d is the coefficient of drag of the diffuser. The bare turbine without the diffuser delivered a value for $C_p=$ 0.43. With the SVR model's predicted optimum diffuser added this value was increased to $C_p=$ 1.67. This corresponds to a factor increase in power of 3.88 over its bare turbine counterpart. However the total system drag was now increased from 283 N to 3194 N representing a factor increase in drag of 11.2. However the new turbine with diffuser produces four times the power and if the drag of four single bare turbines equate to 1132 N a factor increase in drag of 2.8 is found for the same power output of 1417 W.

3.5. Response Surface Modelling

One of the more established metamodelling techniques is response surface modelling (RS). The training data used in the SVR model creation was used to fit a RS model. No adjustment in formulation parameters where necessary and following the same convergence method for the SVR model a optimum based on RS modelling was achieved. The fitment quality and optimum design differed from the SVR model. Table 3 shows the optimum design values.

Table 3: Details of optimum diffuser as determined by RS

C_p	C_d	x_1	x_2	x_3	x_4
1.616	1.828	0.415	0.435	0.455	0.475

For the RS model a standard deviation of 0.104 in C_p values existed whereas for the SVR model the standard deviation was 0.0128. This shows that the fitment quality of the SVR model was superior to the RS model.

3.6. Final Design

The final design of the diffuser used the parameters as established by the SVR model's optimum values. Figure 3. shows the flow domain and contour plot of the axial velocity with a enlarged area of the rotor and diffuser.
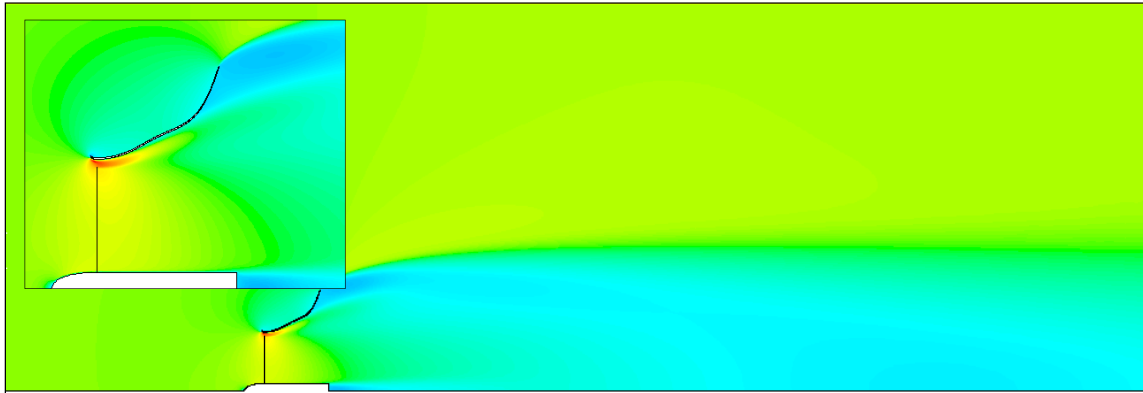

Figure 3: Axial velocity contour plot

The final design showed an axial velocity at the rotor plane of 2.014 m/s compared to the bare turbine rotor plane axial velocity of 1.275 m/s. From the figure it can be seen that a high velocity fluid jet passes between the diffuser and rotor tip. High energy flow is injected into the boundary layer region by the high velocity jet that re-energizes the boundary layer and so prevent the onset of boundary layer separation in the diffuser (Bet 2003). A vertical end part to the diffuser shows the eventual flow separation region. But serving as a flanged part this region has a beneficial effect on power production as shown in (Matsushima et al. 2006).

4.   Design and Manufacturing

Designing of the diffuser incorporated a FEM model of the support structure that was to be used in experimental testing that housed the turbine and diffuser as well as the drive train containing the measurement instruments. Using topology optimization the placement of support struts to minimize structural deflection was obtained. After performing buckling analysis and checking the structural integrity no material failure was predicted by the model and showed a maximum combined stress experienced by the steel support structure to be 93 MPa. A maximum combined stress of 14.7 MPa was experienced by the diffuser with wall thickness of 10 mm.

The diffuser was manufactured using fibreglass and a handlayup process. The materials used where chop strand mat with a density of 450 g/m^2 with a low shrinkage polyester resin. The mould used to perform the hand layup on was manufactured from high density polyurethane foam (40 kg/m^3).

5.   Experimental Investigation

Tests were conducted at the University of Stellenbosch towing tank facility. The towing tank has a length of 90 m width of 4.6 m and depth of 2.3 m. The experimental setup can be seen in figure 4. It shows the electrical braking used by means of a variable speed controlled three-phase motor allowing measurement of the turbine power characteristics over a tip speed ratios (TSR) ranging from 1 to 12. The power produced by the turbine was measured by means of a torque transducer and an optical tachometer. All data were logged using a Spider 8 bridge amplifier and CatmanEasy version 2 software. The torque transducer, tachometer and the towing tank trolley speed were calibrated. Since a drive train was used to transport the power from the turbine shaft to the measurement shaft system losses were measured and accounted for in processing the data. A towing speed of 1.5 m/s was used to simulate the fluid flow velocity.
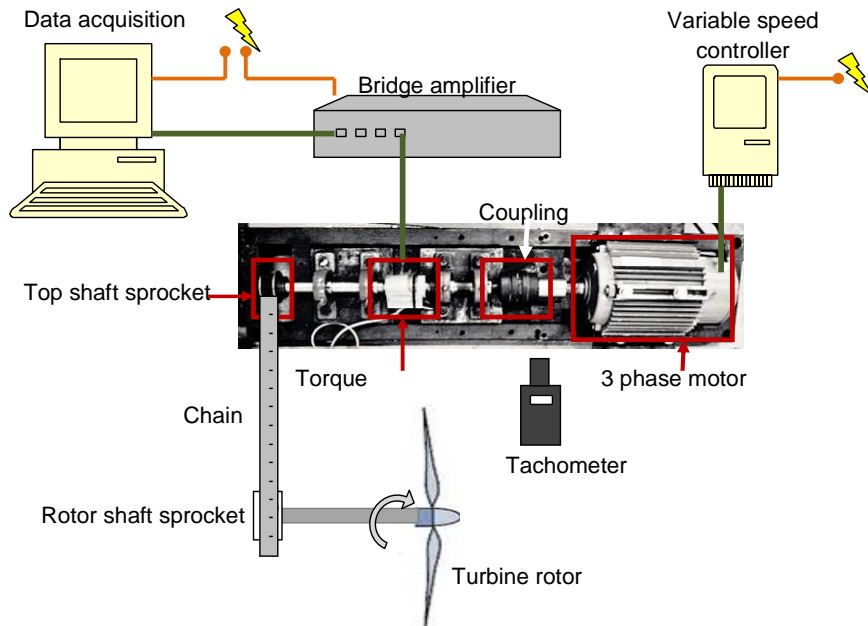
Figure 4: Experimental setup Diagram

The rotor design of Bahaj (Bahaj et al. 2007) was used and had a total blade twist of 15°. A second set of rotor blades used were designed by Stanford(Stanford 2008) that has the same blade section distribution as the Bahaj rotor except having a blade twist of only 10°. Both rotor sets have a diameter of 800 mm and where also used by Grobbelaar (Grobbelaar 2008) in his straight wall diffuser experiments. For the tests the rotor was centred at a depth of 1.2 m and 2.3 m from the sides of the tank.

Figure 5: Experimental setup in the towing tank facility

5.1. Data Reduction and Presentation

For a the given towing tank speed of 1.5 m/s and TSR, the rotational speed (ω) and torque (T) were measured. By varying the motor speed the turbine rotational speed could be controlled and the TSR varied and the power characteristics determined. For the experiments the power coefficient (C_p) and tip speed ratio (TSR) are defined as follow.

Tip speed ratio

$$TSR = \frac{\omega R}{V_0}$$

Power Coefficient

$$C_p = \frac{T\omega}{0.5\rho A V_0^3}$$

Where A is the rotor swept area. Blockage correction for the turbine with the diffuser was not taken into account in the data representation due to different approaches investigated as proposed by (Bahaj et al. 2007) suggesting different values for the blockage correction.

6.   Results and Discussion

Results were recorded for the two rotor sets when used in conjunction with the optimized diffuser. Figure 6 shows the experimental results.
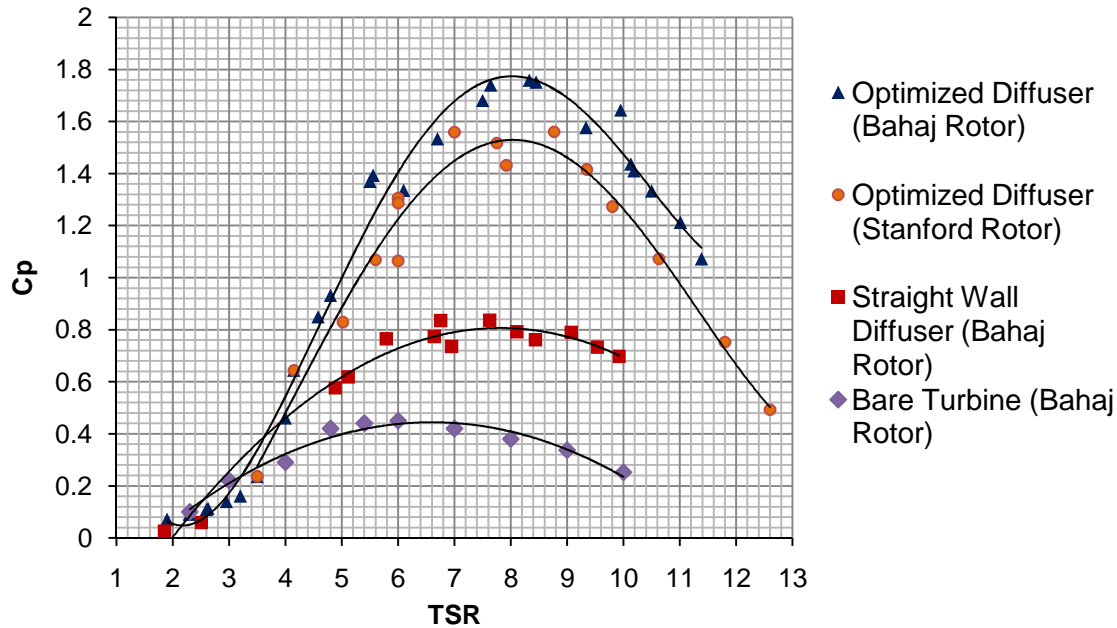

Figure 6: Performance curves of tested turbine and diffuser systems

From figure 6 the optimized diffuser with the Bahaj rotor set produced a maximum C_p = 1.74 compared to the CFD prediction of C_p = 1.672, a overestimation of 4.1%. This over estimation is attributed to the blockage effect that has not been taken into account. Considering that the towing tank had a cross sectional area of 11.95 m^2 and the diffuser 1.64 m^2 , a blockage area ratio of 13.8 % existed. The experimental tests for the straight wall diffuser and bare turbine were also computed without taking into account the effect of blockage correction.Between a TSR of 2-4 it can be seen that the performance of the optimized diffuser is lower than the other data sets. The diffuser was optimized for a single performance point (TSR = 8) and not over the entire flow range. For this reason the boundary layer is adversely affected in the low TSR range and thus separation occurs and impedes the flow of the wake, hence a drop in performance.However as the TSR is increased the diffuser effect is invoked and attachment of the boundary layer occurs and a rapid rise in power is experienced between a TSR 4 and 7. The performance levels out and then reaches a maximum of 1512 W (C_p = 1.74) at a TSR of 8.4. After this point however the pressure gradient becomes excessive behind the rotor and the boundary layer separates from the diffuser wall causing a drop in performance.

For the Bahaj rotor set the straight wall diffuser predicted a C_p = 0.83 and produced a maximum power of 707 W. The power produced from the optimized diffuser (1512 W) is a factor increase of 2.12 over the straight wall diffuser and an factor 4.05 over the bare turbine.

Gaden's (Gaden & Bibeau 2010) straight wall diffuser investigation showed a factor increase in power of 2.875 for an area ratio of 3.29. Thus our study is significant in that the factor increase in power was significantly increased beyond 2.875 for a similar area ratio by use of a optimized curved plate diffuser.

Scaling the results of the bare turbine with no diffuser from 0.4 m diameter to 0.726 m gives a power output of 1227 W. Conversely, a 0.4 m diameter turbine with a 0.726 m optimized diameter diffuser produced 1512 W a factor increase in power of 1.23. Correspondingly if the optimized diffuser's coefficient of power is calculated using the scaled up turbines diameter it computes to C_p = 0.56. Therefore, sacrificing turbine size to include a diffuser seems productive based on results.

An additional benefit of using a smaller turbine with a diffuser as opposed to a larger bare turbine results from the torque generated. The diffuser augmented turbine at its maximum power, generates a smaller torque at higher shaft revolutions. Whereas the bare turbine produces a larger torque at lower shaft revolutions. For this reason a smaller generator can be used on the diffuser turbine whereas the bare turbine needs a bigger generator. However to see if there is any real economical benefit an detailed cost model of both the scaled up bare turbine and the diffuser with a turbine should be conducted to give conclusive answers.

7.   Conclusion

This study investigated the effect of a diffuser on existing rotor models. The use of a 2D axisymmetric CFD simulation utilizing a discontinuous pressure jump to model the turbine rotor was implemented. It was validated against existing 1D turbine theory and a modified Glauert empirical relation.

A CFD model was parameterized to include the geometric design variable describing the diffuser shape and expanded in parallel computing environment to compute the DOE points. Fitment of a SVR and RS model was used to create a metamodel and the built in gradient based optimizer of Matlab used to find the optimum.

It was shown that for a given bare turbine a maximum power increase of a factor 4.05 was achieved by addition of the optimized diffuser.

From CFD estimates the flow speed at the rotor was increased by a factor 1.34. Considering that a ocean or tidal site is selected with a minimum criteria in flow speed of 2 m/s. With the addition of this specific diffuser a flow speed of 1.5 m/s can now be considered for application areas. Thus increasing the application area of where OCTs can be utilized.

This investigation aims to add to the knowledge base of current research into diffuser applications on OCTs and the effect of a specific diffuser on a model OCT rotor has been presented.

References

Bahaj, a., Batten, W. & Mccann, G., 2007. Experimental verifications of numerical predictions for the hydrodynamic performance of horizontal axis marine current turbines. *Renewable Energy*, 32(15), 2479-2490.

Batten, W. et al., 2008. The prediction of the hydrodynamic performance of marine current turbines. *Renewable Energy*, 33(5), 1085-1096.

Bedard, R. et al., 2007. NORTH AMERICAN OCEAN ENERGY STATUS – MARCH 2007. *Energy*, (March), 4-11.

Bet, F., 2003. Upgrading conventional wind turbines Bet, F. and Grassmann, H. Renewable Energy, 2003, 28, (1), 71–78. *Fuel and Energy Abstracts*, 44(3), 162.

Buhl, M.L. & Buhl, M.L., 2005. A New Empirical Relationship between Thrust Coefficient and Induction Factor for the Turbulent Windmill State A New Empirical Relationship between Thrust Coefficient and Induction Factor for the Turbulent Windmill State. *Contract*, (August).

Clarke, S.M., Griebsch, J.H. & Simpson, T.W., 2005. Analysis of Support Vector Regression for Approximation of Complex Engineering Analyses. *Journal of Mechanical Design*, 127(6), 1077.

Fraenkel, P.L., 2007. Marine current turbines: pioneering the development of marine kinetic energy converters. *Proceedings of the Institution of Mechanical Engineers, Part A: Journal of Power and Energy*, 221(2), 159-169.

Gaden, D.L. & Bibeau, E.L., 2010. A numerical investigation into the effect of diffusers on the performance of hydro kinetic turbines using a validated momentum source turbine model. *Renewable Energy*, 35(6), 1152-1158.

Grassmann, H., 2003. A partially static turbine—first experimental results. *Renewable Energy*, 28(11), 1779-1785.

Hansen, M.O., 2008. *Aerodynamics of Wind Turbines* Second., Earthscan.

Igra, O., 1981. Research and development for shrouded wind turbines. *Energy Conversion and Management*, 21(1), 13-48.

Jamieson, P. et al., 2008. Extraction in a Linear Constant Velocity Flow Field. *Energy*, (January), 445-457.

Lee, Y., Oh, S. & Choi, D., 2008. Design optimization using support vector regression. *Journal of Mechanical Science and Technology*, 22(2), 213-220.

Matsushima, T., Takagi, S. & Muroyama, S., 2006. Characteristics of a highly efficient propeller type small wind turbine with a diffuser. *Renewable Energy*, 31(9), 1343-1354.

Rourke, F.O., Boyle, F. & Reynolds, A., 2010. Marine current energy devices: Current status and possible future applications in Ireland. *Renewable and Sustainable Energy Reviews*, 14(3), 1026-1036.

Rourke, F.O., 2009. Tidal Energy Update 2009 — Use Licence —. *Update*.

Viana, F.A., 2009. Surrogates toolbox.

Werle, M.J. & Presz, W.M., 2008. Ducted Wind/Water Turbines and Propellers Revisited. *Journal of Propulsion and Power*, 24(5), 1146-1150.